The Multistep Dissociation of Fluorine Molecules under Extreme Compression

Defang Duan[1], Zhengtao Liu[1], Ziyue Lin[1], Hao Song[1], Hui Xie[1], Tian Cui[2,1,*], Chris J. Pickard[3,4], Maosheng Miao[5,6,†]

[1]*State Key Laboratory of Superhard Materials, college of Physics, Jilin University, Changchun 130012, China*

[2]*Institute of High Pressure Physics, School of Physical Science and Technology, Ningbo University, Ningbo, 315211, People's Republic of China*

[3]*Department of Materials Science & Metallurgy, University of Cambridge, 27 Charles Babbage Road, Cambridge CB3 0FS, United Kingdom*

[4]*Advanced Institute for Materials Research, Tohoku University 2-1-1 Katahira, Aoba, Sendai, 980-8577, Japan*

[5]*Beijing Computational Science Research Center, Beijing 10084, P. R. China*

[6]*Department of Chemistry and Biochemistry, California State University Northridge, California 91220, United States*

Abstract

All elements that form diatomic molecules, such as H_2, N_2, O_2, Cl_2, Br_2, and I_2 are destined to become atomic solids under sufficiently high pressure. However, as revealed by many experimental and theoretical studies, these elements show very different propensity and transition paths, due to the balance of reduced volume, lone pair electrons, and interatomic bonds. The study of F under pressure can illuminate this intricate behavior since F, owing to its unique position on the periodic table, can be compared with H, with N and O, and also with other halogens. Nevertheless, F remains as the only element whose solid structure evolution under pressure has not been thoroughly studied. Using a large-scale crystal structure search method based on first principles calculations, we find that, before reaching an atomic phase, F solid transforms first into a structure consisting of F_2 molecules and F polymer chains and then a structure consisting of F polymer chains and F atoms, a distinctive evolution with pressure that has not been seen in any other elements. Both intermediate structures are found to be metallic and become superconducting, a result that add F to the elemental superconductors.

Many elements, such as H, N, O, and Cl, form diatomic molecules under ambient conditions. At high enough pressure they are destined to transform into atomic phases, accompanied by emerging properties such as metallization and high T_c superconductivity. Being the most abundant element, hydrogen, although containing only one electron in its shell, is very resistant to molecular dissociation and undergoes a series of structure changes before eventually transforming into atomic phases under extremely high pressures (> 550 GPa) [1]. Intermediate phases show complex structural features, such as the coexistence of two types of H. Computational predictions [2,3] and the experimental evidence [4] reveal the corresponding phase contains alternating layers formed by two different types of H_2 molecules.

The dissociation of elementary molecules and transformation into atomic phases is dictated by the number of valence electrons. More electrons delay the formation of atomic phases. B and C are stable as covalent solids under ambient pressures, whereas N, due to its peculiar electron counting, forms the exceedingly strong N≡N triple bonds and the most stable diatomic molecule. However, despite the presence of many metastable phases, its stable molecular phase evolves directly into an atomic "cubic gauche" (cg) phase at a modest pressure of about 110 GPa [5,6]. Its atomic phases show intricate structural variations, such as the predicted N_{10} diamondoid structure at 263 GPa [7] and an all-nitrogen metallic salt at 2.5 TPa [8], respectively. As compared to N, O has 6 valence electrons, a number that is suitable for a double O=O bond and two lone electron pairs on each O. Although O_2 molecules consist of weaker bonds than N_2, counterintuitively, they are much more resistant to dissociation and persist up to 1.9 TPa, beyond which they form polymeric spiral chain and zig-zag chain structures [9,10]. The next element is Fluorine, in which the diatomic bond is the weaker than for both N_2 and O_2, since the number of its valence electrons only permits the formation of single bonds. Nevertheless, no study, theoretical or experimental, has demonstrated the dissociation of F_2 under pressure. The x-ray powder diffraction studies of Meyer et al. indicated that α-F_2 is monoclinic with two candidate space groups $C2/m$ and $C2/c$ of solid fluorine at ambient pressure [11]. Lv

et al performed *ab initio* calculation and found that the *C*2/*m* structure is dynamically unstable, and that the *C*2/*c* structure transforms to *Cmca* above 8 GPa and remains stable up to 100 GPa [12].

The behavior of F_2 molecules under pressure can also be compared with diatomic molecules of other halogens such as Cl_2, Br_2 and I_2. The metallization and dissociation of these molecules have been observed experimentally. Solid molecular I_2 becomes mixed-molecular structure at 12.5 GPa [13], an insulator to metal transition occurs at about 16 GPa keeping molecular characteristic and dissociates into incommensurate modulated structure at about 23 GPa [14]. The incommensurate structure transforms to an atomic phase with space group *Immm* at 30 GPa, then to *I*4/*mmm* at 45 GPa, finally to *Fm*-3*m* phase at 53 GPa [15]. The Cl_2 and Br_2 solids share a common phase transition with I_2, but the transition pressures are higher [16,17]. Recent experiments show that the mixed-molecular structure, metallization and molecular dissociation for Cl_2 occurs at about 130, 200 and 258 GPa, respectively [18]. Remarkably, both I and Br are found to become superconducting with T_c=1.2 K and T_c=1.5 K at 28 and 90 GPa, respectively [19], which are consistent with theoretical predictions [20,21]. Together with metallic hydrogen, these results suggest that superconductivity might be a ubiquitous phenomenon, accompanying molecular dissociation under pressure.

In this letter, we report an unexpected and unique structural evolution of F_2 molecular crystal under high pressure, obtained from extensive structure searches in conjunction with first principles calculations. Strikingly, instead of transforming directly from molecular phases to atomic or extended phases like H, N, and O, Fluorine undergoes transitions into two intermediate structures, one that is stable from 2.8 TPa to 4 TPa consists of both F_2 molecules and polymeric F chains, and the other that is stable from 4 TPa to 30 TPa consists of both F atoms and polymeric F chains. The true atomic phase of F can only be obtained under extremely high pressures beyond 30 TPa, clearly revealing the distinct resistance of F towards transition to an atomic phase. Despite the remaining molecular features in the intermediate structures,

they are found to be superconducting, albeit with low T_c of only a few Kelvin.

The structure prediction is the key to computational materials discovery [22]. We searched for low enthalpy structures of fluorine in the multi-TPa range using the *ab initio* random structure searching (AIRSS) method [23,24]. This approach has been applied to many systems including hydrogen [2,3], oxygen [10] and nitrogen [8] at high pressures. AIRSS based structure predictions were performed at selected pressures of 0.5, 1, 2, 3, 4, 5, 10, 20, 30, 40 TPa and different cell sizes containing up to 30 atoms. The validity of the potentials and the exchange correlation functionals have also been tested, the results are shown in Figs. S1–S3 of Supplemental Material [25]. Details of these computational methods and parameters are provided in the Supplemental Material.

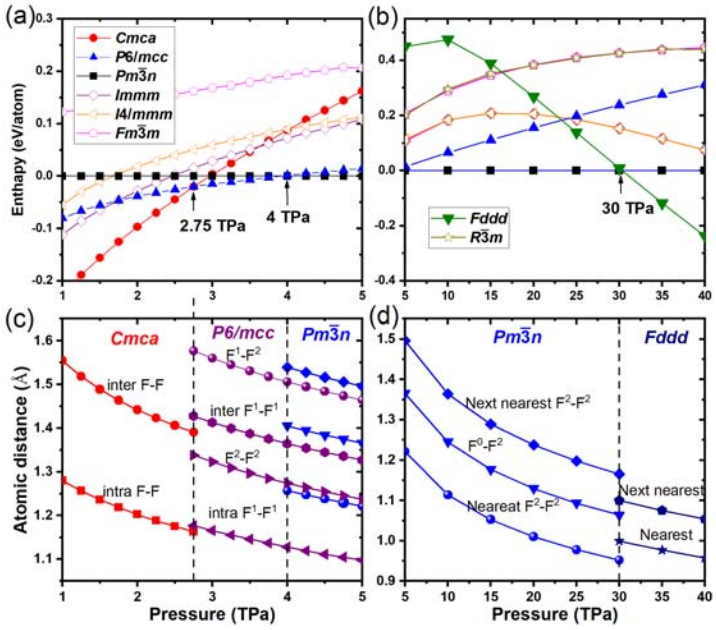

FIG. 1. (color online). (a) and (b) Enthalpies of various structures relative to the $Pm\bar{3}n$ structure as functions of pressure. (c) and (d) The interatomic distances as function of pressure, including the nearest F–F distances (intra F–F) and the next nearest F–F distances (inter F–F) in the *Cmca* phase; the nearest F^1–F^1 distance (intra F^1–F^1), the next nearest F^1–F^1 distance (inter F^1–F^1), the nearest F^2–F^2 distance, and the neighboring F^1– F^2 distance in the *P*6/*mcc* phase; the nearest F^2–F^2 distance, the

neighboring F^0–F^2 distance, the next nearest F^2–F^2 distance in the $Pm\bar{3}n$ phase, the nearest and next nearest F- F distance in the *Fddd* phase.

Figure 1 shows the pressure dependence of enthalpy for structures that are found in this work as well as the most stable structures from previous studies. Strikingly, the molecular *Cmca* phase that was found to be stable from 8 GPa to 100 GPa persists up to 2.75 TPa. The low-pressure molecular phases such as *C*2/*m* and *C*2/*c* are omitted because they are only stable below 8 GPa and their enthalpies are very close to that of *Cmca*. At 2.75 TPa, F transforms from the *Cmca* structure to a *P*6/*mcc* structure and then, at 4 GPa, to a $Pm\bar{3}n$ structure. This structure is surprisingly stable in a large pressure range and only transforms to an *Fddd* structure at 30 TPa. As shown by the calculated phonon spectra (Fig. S4), no structure shows dynamic instability in the pressure ranges that they are predicted to be thermodynamically stable.

Apart from the exceedingly wide range of stable pressures, the structures of these phases show a striking feature, namely the coexistence of atomic, molecular, and polymeric F atoms in the same structure. Although similar abnormal structural features were reported in amorphous N_2 [32] and SO_2 [33] recently, it remains a surprise that all the three different stages of structural evolution of the light p-block elements can coexist in thermodynamically stable crystalline phases. Among four stable structures, *Cmca* is a pure molecular phase and *Fddd* is a true atomic phase. The nearest F-F distances in *Cmca* at 1 TPa are calculated to be 1.28 Å, while the next nearest F-F distances are 1.55 Å, which clearly shows the F_2 molecular character in this structure. For comparison, the bond length of F_2 molecules in gas phase is 1.43 Å. With increasing pressure, both nearest and next nearest F-F distances decrease but the molecular features remain throughout its stable pressure range.

In contrast to the *Cmca* and *Fddd* structures, there are two types of F atoms in the two intermediate structures, F^1 and F^2 in *P*6/*mcc* and F^2 and F^0 in $Pm\bar{3}n$. TheF^1/F^2 and F^2/F^0 ratios are 6:1 and 3:1 in these two structures, respectively. As shown in Fig. 2, *P*6/*mcc* consists of layers of F_2 molecules formed by F^1 atoms;

whereas F^2 atoms form straight polymeric chains that are perpendicular to the F_2 molecule planes. At 3 TPa, the nearest F^1- F^1 distance is 1.17 Å, and the next nearest F^1– F^1 distance is 1.41 Å and is inside the F_2 planes. In contrast, the nearest F^2– F^2 distance in the chain is 1.32 Å, indicating a weaker bond comparing with F^1– F^1. The neighboring F^1– F^2 distance is 1.56 Å, significantly larger than the neighboring distances between F atoms of the same type. Interestingly, the structural motifs of F_2 planes are very similar to several high pressure structures of H_2 [2], such as the $P6_3/m$ and $C2/c$ structures. In particular, the topology of the F_2 planes in $P6/mcc$ structure is identical to that of the H_2 planes in $P6_3/m$ structure (see Fig.2 (b)). The major difference is that the vertical H atoms form H_2 molecules in $P6_3/m$, whereas the vertical F^2 atoms in $P6/mcc$ form linear chains, as shown in Fig. 2 (a).

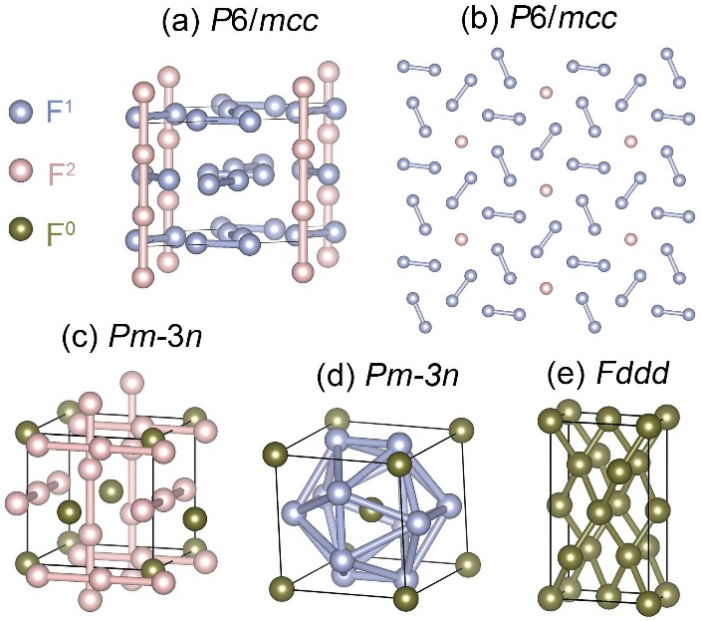

FIG. 2. (color online). (a) The crystal structure and (b) a layer of $P6/mcc$. The F^1, F^2 and F^0 are shown using blue, pink and dark yellow spheres, respectively. The layers are stacked in an ABCBA fashion. The crystal structure of $Pm\bar{3}n$ showing (c) polymeric line chains and (d) icosahedron. (e) The crystal structure of atomic phase $Fddd$.

Although both the $P6/mcc$ and $Pm\bar{3}n$ structures consist of two types of F atoms,

the structural features of the two are distinctly different. Interestingly, $Pm\bar{3}n$ is identical to A15 structures of some binary compounds such as Cr_3Si, except F plays the roles of both constituents in A15. The major difference to the *P*6/*mmc* structure is that there are no F_2 molecules in this structure. This does not mean that F has transformed into an atomic phase, because, as in all A15 structures, the F^2 atoms form polymeric chains, with different bonding features to the F^0 atoms. Correspondingly, at 5 TPa, the nearest F^2– F^2 distance in $Pm\bar{3}n$ structure is 1.22 Å, which is slightly smaller than the F^2– F^2 distance of 1.24 Å in *P*6/*mcc* line chains. Each F^0 atom has 12 neighboring F^2 atoms, with F^0– F^2 distance of 1.37 Å at 5 TPa. The F^2 atoms surrounding the F^0 atom can be viewed as forming a deformed icosahedron. The distance of one edge of the distorted icosahedron is 1.22 Å (the nearest F^2– F^2), and the other edge distance is 1.50 Å (the next nearest F^2– F^2). Such cage structures are common in compounds formed by group 14 elements (C, Si, Ge) at ambient condition, but rarely seen in solids under very high pressures. A well know exception is the N_{10} cage structure in diamondoid nitrogen [7].

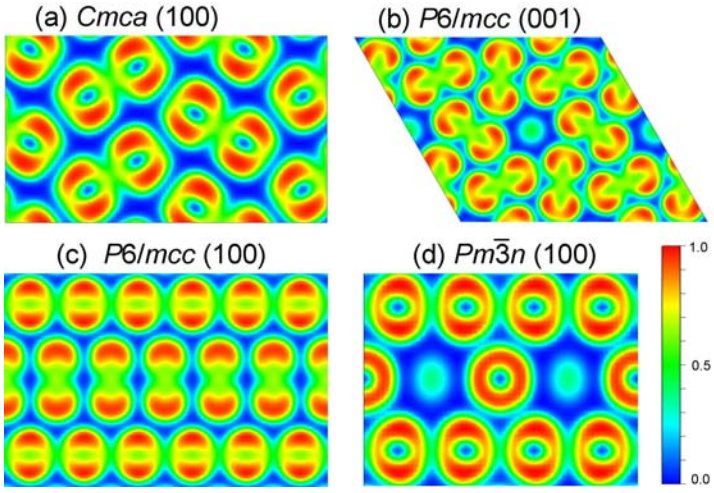

FIG. 3. The calculated ELF of our predicted phases. (a) *Cmca* in the (100) section at 3 TPa. (b) and (c) *P*6/*mcc* in the (001) and (100) section at 3 TPa. (d) $Pm\bar{3}n$ in the (100 section) at 5 TPa.

The mixed molecular and polymeric F in *P*6/*mcc* and mixed polymeric and

atomic F in $Pm\bar{3}n$ structures are also revealed distinctively by their bonding nature. Electron Localization Functions (ELF) can distinguish the bond type and strength and is therefore calculated for the two structures. As shown in Fig. 3, ELF shows not only strong covalent bonds in F_2 molecules in *Cmca* and *P*6/*mcc* structures but also considerably stronger bonds between neighboring F^2 atoms in the line chains in *P*6/*mcc* and $Pm\bar{3}n$ structures. The F^1 atoms in neighboring molecules in the same F_2 plane are also moderately bonded in *P*6/*mcc* structure. On the other hand, ELF values between the F^1 and F^2 atoms in *P*6/*mcc* and the F^0 and F^2 atoms in $Pm\bar{3}n$ are small, indicating weak bonding between them.

The structural evolution of solid F under pressure is accompanied by changes in electronic structure. The molecular *Cmca* phase has a significant electronic gap, that decreases with pressure up to 500 GPa and then increases with pressure throughout its stable pressure range. At 2.75 TPa, the transition pressure to *P*6/*mcc* phase, its gap becomes 2.65 eV as calculated by DFT using the PBE functional. The change of the band gap in *Cmca* structure is the result of the two competing effects. Under increasing pressure, it is reduced by the increasing intermolecular interactions, and increased by the contraction of the F-F bonds. In contrast to the molecular phase, the two intermediate phases, *P*6/*mcc* and $Pm\bar{3}n$, and the atomic phase, *Fddd*, are all metallic. Interestingly, as shown by the projected density of states (PDOS), the F_2 molecules in *P*6/*mcc* contribute significantly to the electron density at the Fermi level, demonstrating that the metallization might happen without regard to the dissociation of F_2 molecules, similar to H_2 and other halogens. Also, at the Fermi level of the *P*6/*mcc* structure, the PDOS of polymeric F (F^2) is very low and the PDOS of the molecular F (F^1) show a dip, both leading to poor metallicity. In contrast, $Pm\bar{3}n$ shows a much higher DOS at the Fermi level, with contributions from both the polymeric F (F^2) and the atomic F (F^0). Furthermore, *Fddd*, as an atomic phase, shows a typical band structure of metals and a high DOS at the Fermi level. We also

calculated the band structure and the density of sates of *P*6/*mcc* using the Hyed-Scuseria-Ernzerhof (HSE06) hybrid functional [34]. Although the results show slight changes, for example, the HSE06 functional opens a small gap at the Γ point; the major features of the electronic structure remain the same. (Fig. S5).

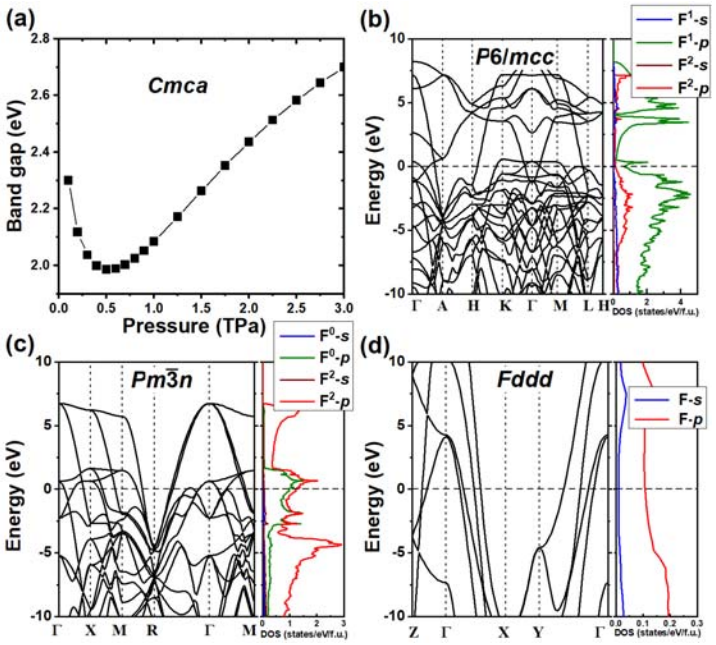

FIG. 4. (color online) (a) Variation of band gaps with pressure for *Cmca*. Band structure and partial densities of states (PDOS) of (b) *P*6/*mcc* phase at 3 TPa, (c) $Pm\bar{3}n$ Phase at 5 TPa, (d) *Fddd* at 30 TPa.

Since the intermediate *P*6/*mcc* and $Pm\bar{3}n$ structures, and the atomic *Fddd* structure are metallic, they are attractive candidates for superconductivity, especially considering that both I and Br become superconducting in their molecular phase. Although the T_c of I and Br are below 2 K, F solids might exhibit higher phonon frequency and stronger electron-phonon coupling because of its lower atomic mass and stronger covalent bonds, both factors might improve T_c. The Eliashberg function, electron-phonon coupling (EPC) constant and logarithmic average phonon frequency ω_{log} are calculated to investigate the superconductivity (Table SI in supplementary information). For *P*6/*mcc* structure, the EPC calculation yields a small λ of 0.29 and a large ω_{log} of 1382 K at 3 TPa. In the case of $Pm\bar{3}n$ and *Fddd* phases, the calculated λ

is 0.38 and 0.44, and ω_{log} is 1923 K and 2224 at 5 TPa and 30 TPa, respectively. The T_c for three phases are calculated using the Allen-Dynes-modified McMillan equation [31]

$$T_C = \frac{\omega_{\log}}{1.2}\exp\left[\frac{1.04(1+\lambda)}{\lambda-\mu^*(1+0.62\lambda)}\right]$$

where μ^* is the Coloumb pseudopotential, with typical values 0.10 and 0.13. The calculated T_c is low at 0.3-1.3 K for the *P*6/*mcc* structure at 3 TPa, 2.1-5.5 K for the $Pm\bar{3}n$ structure at 5 TPa, and 8.4-16.1 K for *Fddd* at 30 TPa. The predicted T_c for atomic phase is larger than that of two intermediate phases, which due to the large λ and ω_{log}.

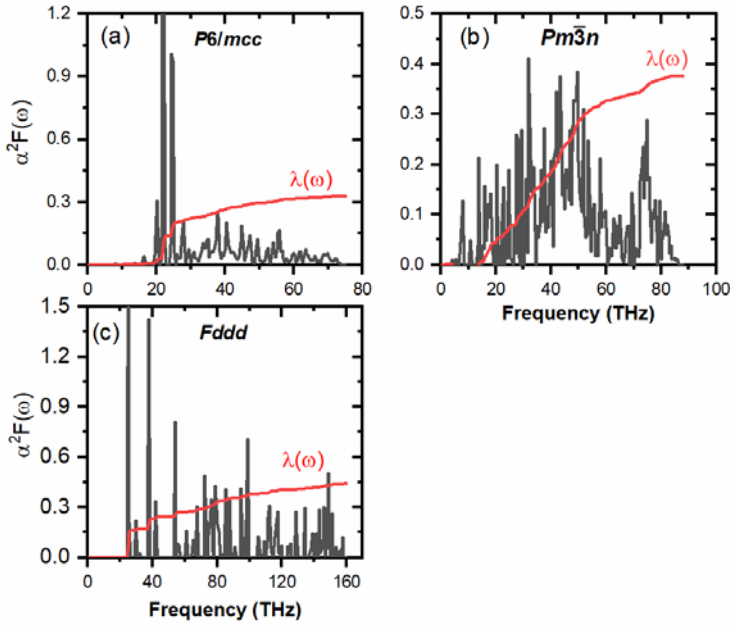

FIG. 5. (color online) The calculated Eliashberg function $\alpha^2F(\omega)$ (black) and EPC coefficient λ (red) of (a) *P*6/*mcc* at 3 TPa, (b) $Pm\bar{3}n$ at 5 TPa, and (c) *Fddd* at 30 TPa.

Finally, we discuss the cause of this unconventional multistep structural evolution toward the complete dissociation of the F-F bonds and the transformation of solid F to the atomic phase. Firstly, the internal energy U and the pV, the two terms of enthalpy, are shown separately as functions of pressure for the four stable structures (see Fig. S6). It reveals that the major driving force for the structure evolution under pressure is the volume reduction. The results reveal very different trend of pV and U under

pressure. Under an increasing pressure up to 5 TPa, the intermediate structures show an improving advantage due to the reduced volume relative to *Cmca* structure. Their internal energies are higher than that of the *Cmca* structure, but the differences dwindle. It is the combination of U and pV that stabilizes these intermediate phases. Between the two intermediate phases, *Pm*-3*n* has smaller volume at both low and high pressures. Its internal energy is higher but becomes smaller than *P*6/*mcc* at 27 TPa. Comparing with these structures, the atomic phase *Fddd* shows a higher internal energy throughout the pressure range. However, its volume and therefore its pV reduces rapidly with increasing pressure. The pV term becomes lower than *P*6/*mcc* at 6 TPa and lower than *Pm*-3*n* at 8 TPa. However, only at 30 TPa, when the reduction in pV overcomes the large excess U, does *Fddd* become the most stable structure. Therefore, the transformation of F to the atomic phase is mainly driven by the volume reduction under pressure. This is in marked difference to H of which the atomic phase is caused by both the volume reduction and the change of the electronic structure.

The intricate structural evolution of F and the general trend of pV and U under pressure is largely due to the competition between reduced volume and the lone pair electrons of F that, compared to all other elements, is the hardest to compress. Although the atomic phase has the smallest volume that favors its formation under pressure, the complete quench of the lone pairs in this structure greatly increases its internal energy. In the pressure range from 2.8 to 30 TPa, F solid compromises the volume reduction and the quench of the lone pairs by adopting the two intermediate structures. In these structures, the lone pairs are only partially quenched because the open interstitial spaces leave room for lone pairs although they are compelled to deform and re-hybridize in these structures. The reduced volume eventually overcomes the large internal energy increase of the atomic structure caused by the quench of the lone pairs, however, the required pressure is much higher than that for other elements, including H and O.

In summary, using a crystal structure prediction method, based on DFT calculations, we have thoroughly studied the structural evolution of solid F under high

pressure and found a unique multistep transformation from low pressure molecular structures to an atomic phase, which has not been seen in any other elementary solid. Comparing with H, N, O and other halogens, F is extremely resistant to becoming an atomic phase and only reaches that destination of all elements under an exceedingly high pressure of 30 TPa. Most strikingly, the structural evolution undergoes two intermediate steps with high-symmetry structures, *P*6/*mcc* and $Pm\bar{3}n$, that contain the mixture of F_2 molecules and F line chains and the mixture of F line chains and F atoms, respectively. Both two intermediate structures and the eventual atomic phase with *Fddd* symmetry are metallic and become superconducting, although the T_c are only at the level of 1 to a few Kelvins.

ACKNOWLEDGEMENTS

This work was supported by the National Key R&D Program of China (No. 2018YFA0305900), National Natural Science Foundation of China (Nos. 11674122, 51632002 and 52072188). CJP acknowledges financial support from the Engineering and Physical Sciences Research Council [Grant EP/P022596/1]. MSM acknowledges the support of NSF CAREER fund (1848141) and the ACS PRF fund (59249-UNI6). Parts of the calculations were performed in the High Performance Computing Center (HPCC) of Jilin University and TianHe-1(A) at the National Supercomputer Center in Tianjin.

Corresponding author：*cuitian@nbu.edu.cn/cuitian@jlu.edu.cn

†miaoms@gmail.com

REFERENCES

[1] J. M. McMahon and D. M. Ceperley, Ground-State Structures of Atomic Metallic Hydrogen, Phys. Rev. Lett. **106**, 165302 (2011).

[2] C. J. Pickard and R. J. Needs, Structure of phase III of solid hydrogen, Nature Phys. **3**, 473 (2007).

[3] C. J. Pickard, M. Martinez-Canales, and R. J. Needs, Density functional theory study of phase IV of solid hydrogen, Phys. Rev. B **85**, 214114 (2012).

[4] R. T. Howie, C. L. Guillaume, T. Scheler, A. F. Goncharov, and E. Gregoryanz, Mixed Molecular and Atomic Phase of Dense Hydrogen, Phys. Rev. Lett. **108**, 125501 (2012).

[5] A. F. Goncharov, E. Gregoryanz, H.-k. Mao, Z. Liu, and R. J. Hemley, Optical Evidence for a Nonmolecular Phase of Nitrogen above 150 GPa, Phys. Rev. Lett. **85**, 1262 (2000).

[6] M. I. Eremets, R. J. Hemley, H.-k. Mao, and E. Gregoryanz, Semiconducting non-molecular nitrogen up to 240□GPa and its low-pressure stability, Nature **411**, 170 (2001).

[7] X. Wang *et al.*, Cagelike Diamondoid Nitrogen at High Pressures, Phys. Rev. Lett. **109**, 175502 (2012).

[8] J. Sun, M. Martinez-Canales, D. D. Klug, C. J. Pickard, and R. J. Needs, Stable All-Nitrogen Metallic Salt at Terapascal Pressures, Phys. Rev. Lett. **111**, 175502 (2013).

[9] L. Zhu, Z. Wang, Y. Wang, G. Zou, H.-k. Mao, and Y. Ma, Spiral chain O_4 form of dense oxygen, Proc. Natl. Acad. Sci. U.S.A. **109**, 751 (2012).

[10] J. Sun, M. Martinez-Canales, D. D. Klug, C. J. Pickard, and R. J. Needs, Persistence and Eventual Demise of Oxygen Molecules at Terapascal Pressures, Phys. Rev. Lett. **108**, 045503 (2012).

[11] T. H. Jordan, W. E. Streib, and W. N. Lipscomb, Single□Crystal X□Ray Diffraction Study of β□Fluorine, J. Chem. Phys. **41**, 760 (1964).

[12] Q. Lv, X. Jin, T. Cui, Q. Zhuang, Y. Li, Y. Wang, K. Bao, and X. Meng, Crystal structures and electronic properties of solid fluorine under high pressure, Chin. Phys. B **26**, 076103 (2017).

[13] Q. Zeng, Z. He, X. San, Y. Ma, F. Tian, T. Cui, B. Liu, G. Zou, and H. k. Mao, A new phase of solid iodine with different molecular covalent bonds, Proc. Natl. Acad. Sci. U.S.A. **105**, 4999 (2008).

[14] T. Kenichi, S. Kyoko, F. Hiroshi, and O. Mitsuko, Modulated structure of solid iodine during its molecular dissociation under high pressure, Nature **423**, 971 (2003).

[15] Y. Fujii, K. Hase, N. Hamaya, Y. Ohishi, A. Onodera, O. Shimomura, and K. Takemura, Pressure-induced face-centered-cubic phase of monatomic metallic iodine, Phys. Rev. Lett. **58**, 796 (1987).

[16] D. Duan, Y. Liu, Y. Ma, Z. Liu, T. Cui, B. Liu, and G. Zou, Ab initio studies of solid bromine under high pressure, Phys. Rev. B **76**, 104113 (2007).

[17] P. Li, G. Gao, and Y. Ma, Modulated structure and molecular dissociation of solid chlorine at high pressures, J. Chem. Phys. **137**, 064502 (2012).

[18] P. Dalladay-Simpson, J. Binns, M. Peña-Alvarez, M.-E. Donnelly, E. Greenberg, V. Prakapenka, X.-J. Chen, E. Gregoryanz, and R. T. Howie, Band gap closure, incommensurability and molecular dissociation of dense chlorine, Nat. Commun. **10**, 1134 (2019).

[19] K. Shimizu, K. Amaya, and N. Suzuki, Pressure-induced Superconductivity in Elemental Materials, J. Phys. Soc. Jpn. **74**, 1345 (2005).

[20] D. Duan, X. Jin, Y. Ma, T. Cui, B. Liu, and G. Zou, Effect of nonhydrostatic pressure on

superconductivity of monatomic iodine: An ab initio study, Phys. Rev. B **79**, 064518 (2009).
[21]D. Duan *et al.*, The crystal structure and superconducting properties of monatomic bromine, J. Phys.: Condens. Matter **22**, 015702 (2010).
[22] A. R. Oganov, C. J. Pickard, Q. Zhu, and R. J. Needs, Structure prediction drives materials discovery, Nat. Rev. Mater. **4**, 331 (2019).
[23] C. J. Pickard and R. J. Needs, High-pressure phases of silane, Phys. Rev. Lett. **97**, 045504 (2006).
[24] C. J. Pickard and R. J. Needs, Ab initiorandom structure searching, J. Phys.: Condens. Matter **23**, 053201 (2011).
[25] See Supplemental Material for computational details, the functionals and pseudopotentials test, phonon dispersion curves, pV and internal energy U with pressure, the calculated Tc and structural information of all predicted structures, which includes Refs. [23, 24, 26-31].
[26] M. D. Segall, J. D. L. Philip, M. J. Probert, C. J. Pickard, P. J. Hasnip, S. J. Clark, and M. C. Payne, First-principles simulation: ideas, illustrations and the CASTEP code, J. Phys.: Condens. Matter **14**, 2717 (2002).
[27]J. P. Perdew, K. Burke, and M. Ernzerhof, Generalized Gradient Approximation Made Simple, Phys. Rev. Lett. **77**, 3865 (1996).
[28] G. Kresse, and J. Furthmüller, Efficient iterative schemes for ab initio total-energy calculations using a plane-wave basis set. Phys. Rev. B **54**, 11169 (1996).
[29] A. Togo, F. Oba, and I. Tanaka, First-principles calculations of the ferroelastic transition between rutile-type and $CaCl_2$-type SiO_2 at high pressures, Phys. Rev. B **78**, 134106 (2008).
[30] G. Paolo *et al.*, QUANTUM ESPRESSO: a modular and open-source software project for quantum simulations of materials, J. Phys.: Condens. Matter **21**, 395502 (2009).
[31] P. Blaha, K. Schwarz, P. Sorantin, and S. Trickey, Full-potential, linearized augmented plane wave programs for crystalline systems, Comput. Phys. Commun. **59**, 399 (1990).
[32] D. Melicherová, O. Kohulák, D. Plašienka, and R. Martoňák, Structural evolution of amorphous polymeric nitrogen from ab initio molecular dynamics simulations and evolutionary search, Phys. Rev. Mater. **2**, 103601 (2018).
[33] H. Zhang *et al.*, Pressure-induced amorphization and existence of molecular and polymeric amorphous forms in dense SO_2, Proc. Natl. Acad. Sci. U.S.A. **117**, 8736 (2020).
[34] A. V. Krukau, O. A. Vydrov, A. F. Izmaylov, and G. E. Scuseria, Influence of the exchange screening parameter on the performance of screened hybrid functionals, J. Chem. Phys. **125**, 224106 (2006).
[35] P. B. Allen and R. C. Dynes, Transition temperature of strong-coupled superconductors reanalyzed, Phys. Rev. B **12**, 905 (1975).